IEEE Access
Multidisciplinary | Rapid Review | Open Access Journal

Date of publication xxxx 00, 0000, date of current version xxxx 00, 0000.

Digital Object Identifier 10.1109/ACCESS.2022.0092316

Simultaneous Placement of Multiple Rooftop Solar PV Integrated Electric Vehicle Charging Stations for Reliability Benefits

GALIVEETI HEMAKUMAR REDDY[1], (Member, IEEE), DEPURU SHOBHA RANI[2], (Member, IEEE), SADHAN GOPE[3], (Senior Member, IEEE), BALLEKURA VEERA NARAYANA[4] and MURALIDHAR NAYAK BHUKHYA[5], (Member, IEEE)

[1]Dept. of Electrical Engineering, DPG Institute of Technology and Management, Gurgaon, Haryana 122004 India (e-mail: ghkr220@gmail.com)
[2]Dept. of Electrical and Electronics Engineering, Institute of Aeronautical Engineering, Hyderabad, Telangana 500043 India (e-mail: depuru_shobha@yahoo.com)
[3]Dept. of Electrical Engineering, National Institute of Technology Agartala, Tripura 799046 India (e-mail: sadhan.nit@gmail.com)
[4]Dept. of Electrical and Electronics Engineering, Aditya Engineering College, Surampalem, Andhra Pradesh 533437 India (e-mail: b.veeranarayana@aec.edu.in)
[5]Dept. of Electrical Engineering, Central University of Haryana, Mahendragarh, Haryana 123029 India (e-mail: rathode.muralidhar@gmail.com)

Corresponding author: Muralidhar Nayak Bhukya (rathode.muralidhar@gmail.com), Shobha Rani Depuru (depuru_shobha@yahoo.com).

ABSTRACT Electric Vehicles (EVs) are known to be future mode of transportation because of their environment-friendly nature. The increase in electric vehicle (EV) penetration needs to set up the new charging stations to meet the demand. The EV charging shows the negative impact on distribution system and system failures lead to the unavailability of power to charge EVs. The EVs not charging due to system failure is to be considered but ignored in the previous studies. Incorporating the Vehicle-to-Grid (V2G) technologies into charging station (CS) improves the system reliability. In this paper, solar rooftop PV units are integrated with CSs to overcome the negative impacts of EV charging and further enhance the reliability of the system. To extracts the maximum benefits from the solar PV integrated charging stations (PVCS), optimal placement is done with objective of reliability improvement. EV reliability is evaluated by using a novel index called as expected energy not charged (EENC). The reliability of both distribution system and EVs are considered as objective functions simultaneously, hence, placement problem becomes multi-objective. The optimal placement is done by considering different EV penetration levels. A multi-objective Grasshopper optimization algorithm (MOGOA) is applied to solve the optimal placement problem of PVCS. The EENS value is improved by 6.18% and 13.9% as compared to base case for case 1 and case 2 respectively. The EENC is improved by 11.51% in case 2 as compared to case 1.

INDEX TERMS Charging station, Distribution system, Electric Vehicles, Grasshopper optimization algorithm, Multi-objective, Optimization, Reliability, Rooftop PV system.

I. INTRODUCTION

IN recent years, distribution systems are undergoing major reinforcements to integrate the distributed generation (DG) and charging stations (CS) for electric vehicles (EVs). The DG integration is a solution to mitigate load growth, improving the system performance and reliability. The EVs are considered as future mode of transportation to reduce the global warming and dependency on fossil fuels. The studies in [1] witnessed that EVs charging during off-peak hours increasing the emission of greenhouse gas (GHG), on the other hand, emission of GHG is reducing if coal-based power generation is removed. Hence, it is clear that if EV batteries are charged using conventional power sources, then the objective of using EVs will not meet. The EVs charging shows potential impact on distribution system performance. Renewable energy sources (RES) are to be integrated to charging stations to mitigate the EVs charging impacts and reduction of GHG emission. The proper placement of RES and EV charging stations enhances the benefits of using RES and EVs.

The integration of RES into the EVs charging station is on rising because of concerns on grid load increase and emission of GHG due to charging of EVs using conventional power sources. Authors in [2] provided a detailed review on technologies used in RES (wind and solar PV) based EV charging stations. The impact of EVs charging on system is nullified with use of wind farms [3]. But wind farms are not recommended to integrate with CSs because of wind power based charging stations are not feasible to use in urban areas. Hence, many researchers are concentrated on solar PV based CSs. Technical reviews are found on solar PV based charging systems and solar PV-grid based CSs [4], [5]. The integration of solar PV system with EV charging stations resulted several benefits. Authors in [6] investigated the use rooftop of parking lots to install EVs charging stations with PV systems. In reference [7], energy losses are minimized by integrating the DGs with charging stations. A study in [8] witnessed that an intelligent energy management and solar PV system are effectively reduced the EV charging impact. The benefits of using solar PV integrated CS are discussed in [9] from the view of economic and environment. Authors in [10] developed PV integrated CS which has reactive power compensation capability. The impact of rooftop solar PV enabled CS on distribution system reliability is discussed in [11]. The power losses are minimized in [12] with the integration of solar rooftop PV system with charging station. A comprehensive review is provided in [13] for rooftop solar PV assisted parking lots for EV charging stations.

From the literature, it is clear that integration of solar PV units with CSs has numerous advantages such as reducing the charging impact during peak hours, reduction in GHG emissions, reliability improvement etc. Lot of research is done on optimal placement of DGs to enhance its benefits considering different objectives in the distribution system. The DGs are placed along with system reconfiguration to enhance the voltage stability [14]. The reconfiguration and DG placement improved the system voltage profile [15]. Power loss is reduced in the system by simultaneously placing the DGs and FACTS [16]. The DGs helped to reduce the energy loss and maximized the cost savings [17]. In ref [18], DG placement enhanced the distribution system resiliency. Authors in [19] enhanced the capability to restore the critical loads during natural disasters with the help of DGs. Distribution system reliability is improved by optimally placing DGs by considering energy not supplied (ENS) as objective function [20].

The researchers also concentrated on optimal placement of CS to enhance the benefits. The optimal placement of CS is done in [21] for cost benefits such as minimization of investment, operating cost and emission cost. Authors in [22], optimally placed CSs by considering multiple objective functions such as power losses minimization, voltage deviation reduction, and maximization of voltage stability index. The performance of system is assessed [23] by optimally placing the PV system and CS simultaneously. Authors in [24], optimally placed the DGs and charging station for reliability improvement but placed them separately.

In the recent literature, it is found that CSs are placed along with DGs by considering multiple objective functions. Authors in [25], DG integrated CSs are optimally placed by considering total system cost, voltage deviation and energy not supplied as objective functions. Minimization of waiting time and annal total cost are considered as objective functions in [26]. Authors in [27], considered there different objective function such as voltage deviation, energy loss and EV owners dissatisfaction for optimal placement of DG integrated CSs. In [25]–[27], solar and wind energy system are used as DGs. In ref [28], CSs are optimally placed in a distribution system integrated with randomly placed solar rooftop PV system by considering active and reactive power loss, voltage deviation and voltage stability index.

It is clear that the integration of DGs and EVs are rising due to their technical and environmental benefits which necessitate the simultaneous planning of DGs and CSs. Researchers are less concerned about reliability of distribution system during simultaneous placement of solar PV integrated charging stations (PVCS). A novel reliability index is developed in [11] to measure the EVs reliability i.e., expected energy not charged (EENC). Authors are claimed that EENC plays a key role for selection of charging station locations. The consideration of EENC as an objective function is not explored yet.

In this work, the charging stations are integrated with solar rooftop PV units to mitigate the EVs charging impact and enhance EVs benefits. The PVCS placement problem is formulated as multi objective i.e., using system reliability and EV reliability as objectives. The expected energy not supplied (EENS) is considered to measure the system reliability and EENC for EV reliability. The PVCS placement problem is solved using Multi-objective Grasshopper optimization algorithm (MOGOA) [29]. Different EV penetration levels are considered for PVCS placement. A coordinated charging and discharging strategy is presented for charging station control during distribution system failures. Two types of V2G modes i.e., scheduled and unscheduled V2G mode. The unscheduled V2G mode only contributes for EENC calculations. The proposed methodologies are applied on a practical Indian distribution system.

The novelty of the paper is as follows:

- Rooftop PV systems are integrated with EV charging stations to mitigate the EV charging impacts from reliability prospective.
- A novel objective function i.e., EENC is introduced for optimal PVCS placement. The EENC consideration is very critical because more EENC leads to the dissatisfaction of EV owners.
- A coordinated charging and V2G strategy is developed and used for charging and discharging of EVs during system faults. This strategy helps to improve the both system and EV reliability.
- PVCS placement problem is formulated as a multi objective problem by considering EENS and EENC as

objective functions.
- Multi-objective Grasshopper optimization algorithm is used to solve optimal PVCS placement problem.
- PVCS impact is analysed for three different EV penetration levels. This analysis is very crucial because number of EVs increases year by year and it is important to know how existing system is impacted with increased EVs.

The remaining sections of the manuscript are as follows: the modelling of EV charging station is discussed in section II which included the modelling of solar rooftop PV units, battery charger and EV modes. Section II also discusses the PV integration to charging station and coordinated charging strategy. In section III, optimal PVCS placement is discussed which includes formulation of objective function, different constraints and optimization technique i.e., grasshopper optimization algorithm. The results are discussed in section IV and finally, the findings concluded in section V.

II. MODELLING OF EV CHARGING SYSTEM

In this work, the proposed charging station mainly consist of three parts i.e., solar rooftop PV units, EVs and battery charger. Schematic diagram of the proposed charging station is shown in Fig. 1. The integration of solar rooftop PV units into the charging station reduces the pressure on the distribution system and increases the reliability of distribution system and EVs as well. The modelling of these three parts is discussed in this section. In Fig. 1, the direction of arrows shows the power flow direction among the solar PV units, charging station, EVs and grid.

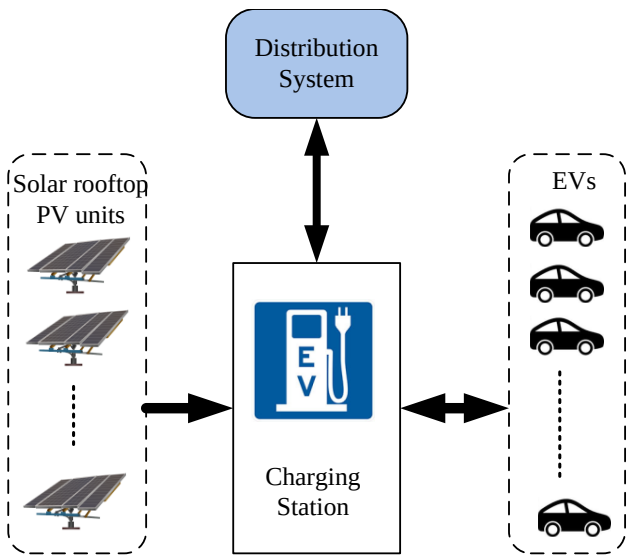

FIGURE 1. Schematic diagram of EV charging station with solar rooftop integration

A. SOLAR ROOFTOP PV UNITS

If an EV is charged through renewable energy source, it increases the benefits of EV usage as the objective is to reduce the GHG emissions. The EV charging stations are mainly situated in highly populated urban areas where the availability of land for renewable sources is a difficult task. In this work, rooftops of commercial and residential buildings are used to install the solar PV units and the output power is supplied to the charging station for EVs charging. The PV output power is highly intermittent and depends on the solar irradiance. The uncertainty of solar irradiance is modelled using beta probability distribution function [30]. The probability density function (pdf) of solar irradiance is expressed as

$$F(s) = \begin{cases} \dfrac{\Gamma(\alpha+\beta)}{\Gamma(\alpha)\Gamma(\beta)} s^{(\alpha-1)}(1-s)^{(\beta-1)} & 0 \le s \le 1, \\ & \alpha, \beta \ge 0 \\ 0 & \text{otherwise} \end{cases} \quad (1)$$

here, Γ= gamma function
s= random solar irradiance in kW/m^2
α , β= shape parameters of beta distribution function

The cumulative distribution function (cdf) of solar irradiance s is expressed as

$$f(s) = \int_0^t F(s) \quad (2)$$

$$= \frac{\Gamma(\alpha+\beta)}{\Gamma(\alpha)\Gamma(\beta)} \int_0^t s^{(\alpha-1)}(1-s)^{(\beta-1)} \quad (3)$$

The probability of solar irradiance being between s_1 and s_2 can be obtained as.

$$f(s_1 < s < s_2) = f(s_2) - f(s_1) \quad (4)$$

The PV cell output power at any state y is determined using following expression.

$$P_{out}(s) = N * f_f * V_y * I_y \quad (5)$$

here, f_f is the fill factor and N is the number of cells in the PV module. The values of f_f , V_y and I_y are calculated using equations available in [31].

B. BATTERY CHARGER

The equivalent circuit of the battery charger is illustrated in Fig. 2 and the battery is represented as a capacitor in the circuit.

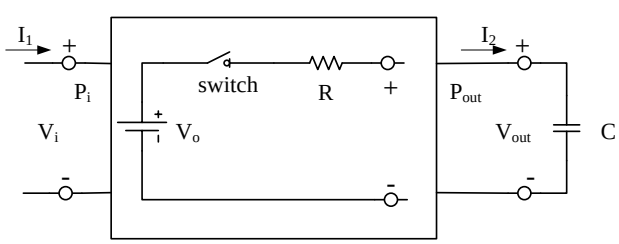

FIGURE 2. Equivalent circuit of a battery charger [11]

The capacitor starts charging at $t = 0$, the Kirchhoff's voltage law is applied on equivalent circuit [11]

$$\begin{aligned} V_o &= V_R(t) + V_{out}(t) \\ &= i(t)R + \eta_r V_c \end{aligned} \tag{6}$$

here, η_r is the charger efficiency. V_o is the charger output voltage. $V_R(t)$ and $i(t)$ are the instantaneous voltage across R and current in R respectively. V_c is the voltage across the capacitor and is determined by

$$V_c = \frac{1}{C}\int_0^t i(\tau)d\tau \tag{7}$$

From the equations (6) and (7)

$$V_o = V_R(t) + \frac{\eta_r}{C}\int_0^t i(\tau)d\tau \tag{8}$$

Differentiate the equation (8) and multiply by C/η_r to get the first order differential equation

$$0 = \frac{RC}{\eta_r}\frac{di(t)}{dt} + i(t) \tag{9}$$

Now, initial condition is applied to equation (6) i.e., $t = 0$, voltage across the capacitor is zero and the initial current i_o is derived by

$$i_o = V_o/R \tag{10}$$

The differential equation (9) is solved to get the instantaneous current $i(t)$ using the initial conditions

$$i(t) = \frac{V_o}{R}e^{-\eta_r \frac{t}{\tau_o}} \tag{11}$$

here, τ_o is the time constant of the charger and $\tau_o = RC$. From the equations (6) and (11), the voltage across the capacitor $V_{out}(t)$ is determined by

$$V_{out}(t) = V_o\left(1 - e^{-\eta_r \frac{t}{\tau_o}}\right) \tag{12}$$

If the capacitor has some initial voltage (V_{int}) then the above equation becomes

$$V_{out}(t) = V_o\left(1 - e^{-\eta_r \frac{t}{\tau_o}}\right) + V_{int} \tag{13}$$

Multiplication of $V_{out}(t)$ by $i(t)$ gives the output power P_{out} and is as follows

$$P_{out}(t) = P_{max}\left(1 - e^{-\eta_r \frac{t}{\tau_o}}\right) + P_{int} \tag{14}$$

here, $P_{max} = V_o \times i(t)$, $P_{int} = V_{int} \times i(t)$ and $t \in (0, t_{req}]$, t_{req} is the required time to get the full charge.

C. EV MODELLING

The EVs are operated in two modes. Charge mode when battery of EV is being charged and V2G (generation) mode when battery of EV is being discharged i.e., injecting energy into the system. In this scenario, V2G enabled charging stations works as energy storage system. Batteries in EVs uses chemical storage, and chemical process follows exponential function over the time during charge/discharge.

1) Charge mode

During the charge mode, EV batteries acts as loads on the system. The instantaneous battery power status ($P_{EV}(t)$) is evaluated by [11]

$$P_{EV}(t) = P_{EV,max}\left(1 - e^{-(\alpha.t/t_{max})}\right) + P_{EV,int} \tag{15}$$

here, α is the charging constant of EV battery. $t \in [0, t_{req}]$ and t_{req} = time required to attain the full charge of EV. $P_{EV,max}$ is the capacity of EV battery. $P_{EV,int}$ is the EV battery initial power status. t_{max} is the required time to full charge from zero power status and is evaluated by $t_{max} = 1/R_C$ (R_C is the charging rate).

The value of t_{req} depends on the initial battery power status and is determined by [11]

$$t_{req} = \begin{cases} t_{max} & ;\text{if } P_{EV,int} = 0 \\ 0 & ;\text{if } P_{EV,int} = P_{EV,max} \\ -\frac{t_{max}}{\alpha} ln\left(\frac{P_{EV,int}}{P_{EV,max}}\right) & ;\text{if } 0 < P_{EV,int} < P_{EV,max} \end{cases} \tag{16}$$

Now, final power status of EV battery depends on t_{req} and calculated by [11]

$$P_{EV}(t) = \begin{cases} P_{EV,max}\left(1 - e^{\frac{-\alpha.t}{t_{max}}}\right) + P_{EV,int} & ;\text{If } t < t_{req} \\ P_{EV,max} & ;\text{If } t \geq t_{req} \end{cases} \tag{17}$$

The total power demand ($P_{EV,dem}$) (required power for full charge) of a EV at time t is calculated as:

$$P_{EV,dem}(t) = P_{EV,max} - P_{EV}(t) \tag{18}$$

Substitute $P_{EV}(t)$ value in eq. (18) to get $P_{EV,dem}(t)$

$$P_{EV,dem}(t) = \begin{cases} P_{EV,max}e^{-\alpha \frac{t}{t_{max}}} - P_{EV,int} & ;\text{If } t < t_{req} \\ 0 & ;\text{If } t \geq t_{req} \end{cases} \tag{19}$$

The effect of a system failure on EV charging is depicted in Fig. 3. At hour t_1, EV is connected to charging station for charging and scheduled to leave at hour t_2 and takes t_{req} for full charging ($t_2 = t_1 + t_{req}$). But, charging is interrupted at hour t_3 due to a failure in the distribution system. Main grid is not available and generation from solar PV units are unable to meet the charging station demand. Now, the power status of the EV battery at hour t_3 is determined by

$$P_{EV,t_3} = P_{EV,max}\left(1 - e^{-\frac{\alpha.(t_3 - t_1)}{t_{max}}}\right) + P_{EV,int} \tag{20}$$

However, the power supply is restored to charging station at hour t_4. Here, two different situations will occur. In situation 1, power is restored after scheduled departure of EV and the battery status is remains same as at hour t_3. On the other hand, in second situation, power is restored before the scheduled departure then battery starts charging again. The duration of battery charging and not charging

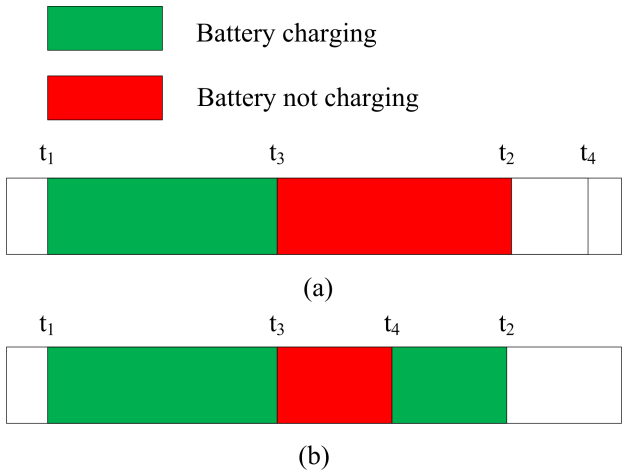

FIGURE 3. Battery charging scenarios a) Situation 1 b) Situation 2

are pictorially shown in Fig. 3 for both the situations. Now, the final power status of EV battery at hour t_2 for second situation is determined by [11].

$$P_{EV,t_2} = \begin{cases} P_{EV,max}\left(1 - e^{\frac{-\alpha.t_{c,r}}{t_{max}}}\right) + P_{EV,t_3} & ;\text{If } t_{c,r} < t_{req} \\ P_{EV,max} & ;\text{If } t_{c,r} \geq t_{req} \end{cases} \tag{21}$$

here, $t_{c,r}$ is the charging time after the restoration of the power supply and $t_{c,r} = t_2 - t_4$, the value t_{req} is re-evaluated considering the battery power status at hour t_3. Now, the power is not charged ($P_{EV,req}$) by an EV due to system failure is determined by

$$P_{EV,req} = \begin{cases} P_{EV,max} - P_{EV,t_3} & ;\text{If } t_4 \geq t_2 \\ P_{EV,max} - P_{EV,t_2} & ;\text{If } t_4 < t_2 \end{cases} \tag{22}$$

The energy not charged by an EV is determined by

$$E_{EV,req} = \begin{cases} \int_0^{t_2 - t_3} P_{EV,req} dt & ; t_4 \geq t_2 \\ \int_0^{t_4 - t_3} P_{EV,req} dt & ; t_4 < t_2 \end{cases} \tag{23}$$

The EV battery power status is given in Fig. 4 for different conditions such as battery charging constant (α), different battery initial power level and different charging rates.

2) V2G mode

In this mode, EVs inject power into the grid. The power status during discharge at time t by a EV is given by

$$P_{EV,dis}(t) = P_{EV,int}.e^{-\beta\frac{t}{t_{max}}} - P_{EV,crit} \quad ; \quad t \in [0, t_{ava}] \tag{24}$$

here, β = battery discharge constant.
$P_{EV,crit}$ = critical power level i.e., minimum level until discharge of EV is allowed.
t_{ava} = duration of EV availability for discharge purpose.
The value of t_{ava} depends on the battery initial power status and critical power level. If t reaches to t_{ava} then $P_{EV,dis}$ becomes zero. Now, substitute these values in eq. (24)

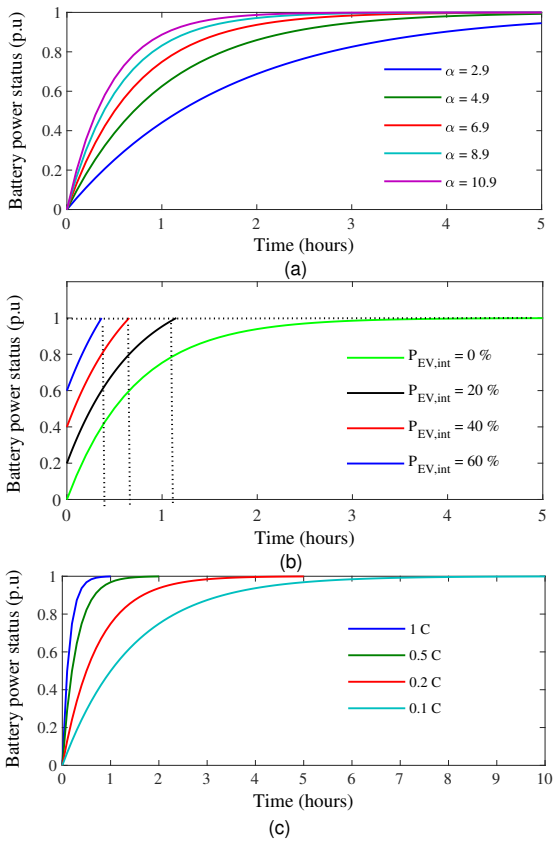

FIGURE 4. EV battery charge status (a) With different battery charging constants (b) With different initial battery levels (c) With different charge rates

$$0 = P_{EV,int}.e^{-\beta\frac{t_{ava}}{t_{max}}} - P_{EV,crit} \tag{25}$$

The above equation is simplified to get the t_{ava} and is as follows

$$t_{ava} = -\frac{t_{max}}{\beta} ln\left(\frac{P_{EV,crit}}{P_{EV,int}}\right) \quad ; P_{EV,crit} < P_{EV,int} \tag{26}$$

Total available power ($P_{EV,ava}$) for discharge is given by

$$P_{EV,ava} = P_{EV,int} - P_{EV,crit} \tag{27}$$

An EV is starts discharging at t_1 hour and system main supply is restored at t_2, now the total power injected by an EV to the system is calculated by

$$P_{EV,inj} = \begin{cases} P_{EV,ava} & ;\text{if } (t_2 - t_1) \geq t_{ava} \\ P_{EV,int}\left(1 - e^{-\beta\frac{(t_2 - t_1)}{t_{max}}}\right) & ;\text{if } (t_2 - t_1) < t_{ava} \end{cases} \tag{28}$$

Let's consider, t_s is the duration of power injected to grid. The total energy injected is calculated by

$$E_{EV,inj} = \int_0^{t_s} P_{EV,int}\left(1 - e^{-\beta\frac{t}{t_{max}}}\right) dt \quad ; t_s \leq t_{ava} \tag{29}$$

D. PV INTEGRATED CHARGING STATION

The solar rooftop PV system is integrated with CS and called as PV integrated charging station (PVCS). The PVCS mitigates the EV charging impacts on the distribution system. The charging/discharging behaviour of PVCS is different from conventional CS as PV systems are integrated with CS. The PV integration enables the CS for its own generation like prosumer. The charging demand for all EVs connected in charge mode at time t is calculated [11]

$$P_{cha,dem}(t) = \sum_{i=1}^{N_c} P^i_{cha,req}(t) \tag{30}$$

N_c is the total EVs in charge mode. $P_{cha,req}(t)$ is the power requirement to charge i^{th} EV at time t and is calculated by using

$$P^i_{cha,req}(t) = \begin{cases} P^i_{EV,max} e^{-\alpha \frac{t_{c,i}}{t^i_{max}}} & ;\text{If } t_{c,i} < t^i_{req} \\ 0 & ;\text{If } t_{c,i} \geq t^i_{req} \end{cases} \tag{31}$$

here, t^i_{max} is the maximum time required for fully charging i^{th} EV. $t_{c,i}$ is the duration of i^{th} EV charging since charging started. t^i_{req} is the required time for i^{th} EV to fully charge under given initial condition of EV battery. $P^i_{PEV,max}$ is the maximum battery capacity of i^{th} EV.

The battery chargers in the PVCS are enabled to operate in V2G mode. The V2G mode of the EVs will helps to reduce the system load during the peak hours and this feature also enables the EVs participation in the demand response programs. The power injected by all the V2G mode EVs at time t is calculated by

$$P_{V2G,gen}(t) = \sum_{i=1}^{N_s} P^i_{V2G,inj}(t) \tag{32}$$

here, N_s is the total number of vehicles in the V2G mode.

The power injected ($P^i_{V2G,inj}$) by i^{th} EV is calculated by

$$P^i_{V2G,inj}(t) = \begin{cases} 0 & ;\text{if } t_{d,i} \geq t_{ava} \\ P^i_{EV,int} e^{-\beta \frac{t_{d,i}}{t^i_{max}}} & ;\text{if } t_{d,i} < t_{ava} \end{cases} \tag{33}$$

here, $P^i_{EV,int}$ is the initial power status of i^{th} EV. $t_{d,i}$ is the discharge time of i^{th} EV since discharge started.

The output power from the rooftop PV system is depends on the weather condition i.e., solar irradiance value (as explained in section II-A). Hence, the PVCS power requirement for charging EVs changes accordingly. The net demand of PVCS is calculated by

$$P_{cha,net}(t) = P_{cha,dem}(t) - P_{V2G,gen}(t) - P_{PV}(t) \tag{34}$$

here, $P_{cha,net}(t)$ is the net power demand of the PVCS at time t. $P_{PV}(t)$ is the output power of the rooftop PV system at time t.

The value of $P_{cha,net}$ defines the mode of PVCS operation i.e., charge and generation modes for positive and negative values respectively.

E. COORDINATED CHARGING

Different parameters in charging stations are uncertain in nature. The uncertain parameters in charging station include EV charging, discharging, charging mode to driving mode and PV output power. These parameters need to be coordinated to satisfy the EV owner charging requirements and balance the load on the distribution system. The flow chart of the proposed coordinated charging algorithm is shown in Fig. 5. The algorithm shown in Fig. 5 is applicable for both normal and system failure conditions.

During system normal operating conditions, all the EVs that are connected in the charge mode are charged seamlessly. But, charging rates are coordinated based on the available PV output, load on the distribution system and scheduled journey. The V2G mode EVs will inject the power as per their scheduled plan. There is no unscheduled injection of power from the EVs during normal operating conditions because the main grid is available to meet the charging and system load demand. However, charging and discharging completely change during the system failures. The main grid supply may not be available during the system failures to meet the charging and system loads demand. Only PV output and power from V2G mode are available to meet the demand and hence, charging of EVs is prioritized based on their current battery power levels and their journey schedule. The journey schedule has direct impact on the battery power level of EV need to keep before leaving the PVCS. For example, the EV which is having a planned trip within one hour has to keep the minimum required battery level (P_{min}) for its scheduled journey. This limit will enable the PVCS to charge the vehicles which are not meeting their minimum requirement. There is an unscheduled power injection from V2G mode of EVs which are having more battery power levels than required and are also subject to EV owners' willingness to participate in the unscheduled V2G mode. This leads to the different power level constraints for different EVs. If the EVs do not have a planned trip within one hour then EVs are charged based on the critical battery level i.e., $P_{EV,crit}$. Fast charging is preferred for EVs those batter levels are below the critical level otherwise standard charging is preferred based on the available power.

III. OPTIMAL PVCS PLACEMENT

In this work, a new objective function i.e., EENC is proposed which reflects the EV reliability and used along with the system reliability index i.e., EENS. The PVCS placement problems is formulated as a multi-objective problem and solved using the multi-objective grasshopper optimization algorithm. In this section, formulation of objective functions, different constraints used during the optimization and working of optimization algorithm are explained in detailed manner.

A. OBJECTIVE FUNCTION FORMULATION

As charging of EVs adds some load to the distribution system, on the other hand, V2G mode supplies power to the

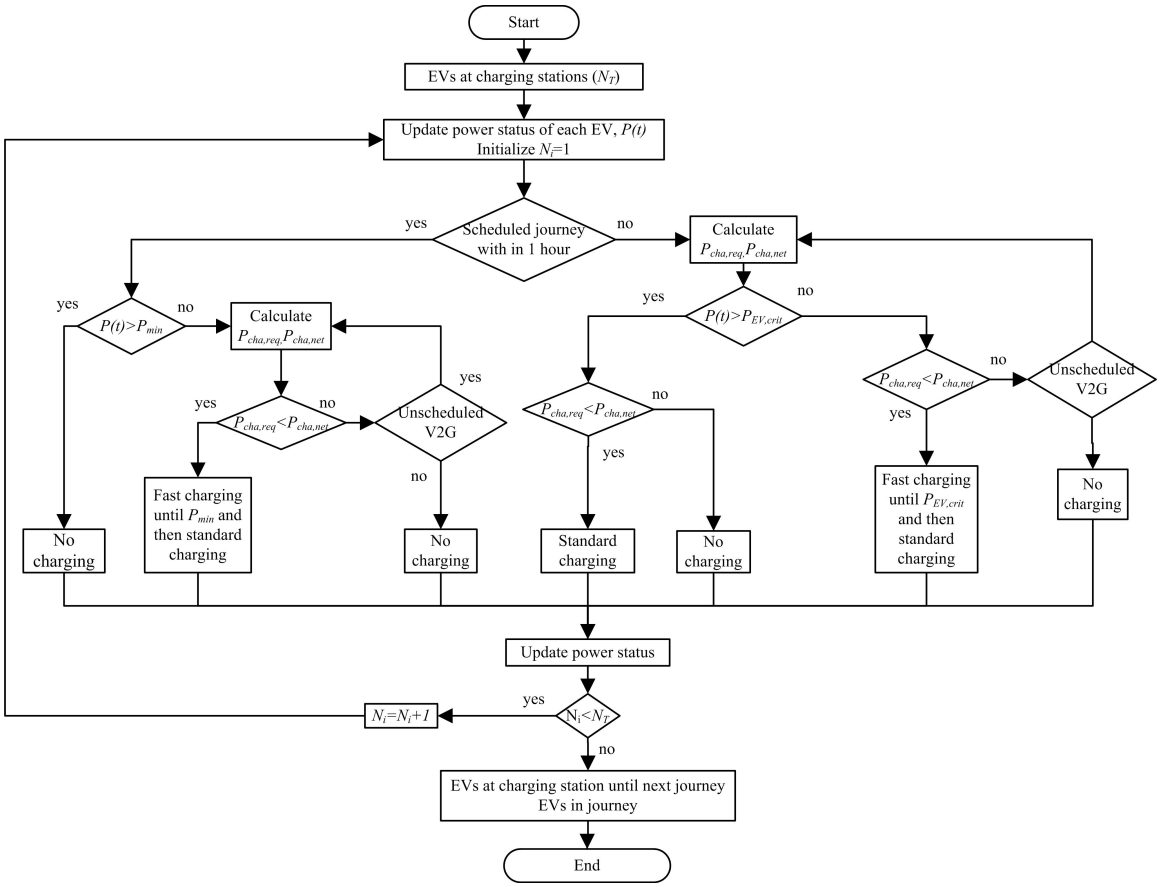

FIGURE 5. EVs charging and V2G strategy with solar rooftop units during a system failure

system. Hence, EVs are considered as special load on the system which have generating capacity. It is a wise decision to consider EVs reliability in the reliability analysis. In this paper, the PVCS placement problem has two objectives i.e., improving the system reliability and EVs reliability.

In order to improve the system reliability, EENS is considered as the objective function and is evaluated as follows

$$EENS = \sum_{j}^{NL} ENS_j \tag{35}$$

$$ENS_j = \sum_{j}^{NO} L_{n,j} U_{n,j} \tag{36}$$

here, NL= Number of load points. NO= Number of Outages for j^{th} load point. $L_{n,j}$=Load on j^{th} load point during n^{th} outage. $U_{n,j}$ = outage duration for j^{th} load point during n^{th} outage.

Index EENC is proposed in [11] to evaluate the reliability of the EVs. The EENC is evaluated in two parts, Energy loss during the charging mode ($EENC_{cha}$) and energy loss due to the unscheduled V2G mode ($EENC_{V2G}$). The $EENC_{cha}$ is evaluated by

$$ENC^i_{cha} = \sum_{k=1}^{N_{i,c}} E^{i,k}_{EV,req} \tag{37}$$

$$EENC_{cha} = \sum_{i=1}^{NV_c} ENC^i_{cha} \tag{38}$$

here, ENC^i_{chr} is the energy not charge by i^{th} EV. $E^{i,k}_{EV,req}$ is the energy not charged by i^{th} EV in k^{th} interruption. $N_{i,c}$ is number of interruptions i.e i^{th} EV charging is affected. NV_c is the total number of EVs effected due to system failures.

The $EENC_{V2G}$ is evaluated by

$$ENC^i_{V2G} = \sum_{k=1}^{N_{i,d}} E^{i,k}_{EV,inj} \tag{39}$$

$$EENC_{V2G} = \sum_{i=1}^{NV_d} ENC^i_{V2G} \tag{40}$$

here, ENC^i_{V2G} is the energy loss of i^{th} EV due to V2G mode. $E^{i,k}_{EV,inj}$ is the energy injected by i^{th} EV during k^{th} interruption. $N_{i,d}$ is number of interruptions i.e i^{th} EV is operated as unscheduled V2G. NV_d is the total number of vehicles operated in unscheduled V2G mode.

Total EENC is determined by

$$EENC = EENC_{cha} + EENC_{V2G} \tag{41}$$

The objective of the system is to improve the reliability of the system and EVs. The objective functions for optimal PVCS placement are as follows

$$obj1 = min(EENS) \tag{42}$$
$$obj2 = min(EENC) \tag{43}$$

B. CONSTRAINTS

1) Operational constraints

The distribution system operation is subject to network constraints such as voltage limits ad thermal limits which are given by

$$V_j^{min} \leq V_j \leq V_j^{max} \tag{44}$$
$$I_i \leq I_i^{max} \tag{45}$$

System stable operation is subject to power flow constraints such as generator active and reactive power limits and power balance. The generator limits are given by

$$P_i^{min} \leq P_i \leq P_i^{max} \tag{46}$$
$$Q_i^{min} \leq Q_i \leq Q_i^{max} \tag{47}$$

The power balance with EV charging is given by

$$P_G = P_D + P_{cha,net} + P_{Loss} \tag{48}$$

here, P_G, P_D and P_{Loss} are the total power generation, power demand and power losses respectively. $P_{cha,net}$ is calculated using eq.(34). $P_{cha,net}$ is positive when CS needs power from the distribution system means PVCS works as a load to the system. $P_{cha,net}$ is negative when PVCS has surplus power and acts as a generator to the system.

There is no constraint on PVCS operating mode during normal operating conditions because load is balanced by the main grid. If main grid is not available due to failures, then PVCS operating mode is very crucial to restore the load by forming the microgrid Microgrids are formed with the help of PVCS after isolating the faulted sections. However, restoration of loads in the microgrid are subject to the mode of PVCS operation i.e., the PVCS is must be in generation mode. Mathematically, it is written by

$$P_{cha,net} < 0 \tag{49}$$

2) EV charging and discharging constraints

The V2G mode EVs will inject the power until it reaches its predefined minimum battery level for scheduled V2G mode EVs under normal operating conditions. During system failures, some of the EVs that are in charge mode are shifted to V2G mode. This V2G mode is called as unscheduled V2G mode of operation. The charging rate must be decided based on the availability of PV output and main grid. All this will put certain constraints while charging and discharging of EV batteries. The constraints are mathematically represented by

$$P_{EV,crit} < P_{EV,pre} \geq a_1 \cdot P_{EV,max} \tag{50}$$
$$P_{cha,net} \leq 0 \tag{51}$$
$$P_{EV,pre} \geq a_2 \cdot P_{EV,max} \tag{52}$$
$$P_{EV,pre} \geq a_3 \cdot P_{EV,max} \tag{53}$$

here, $P_{EV,pre}$ is the present battery power level of the EV that is connected to PVCS. a_1, a_2 and a_3 are the percentage of battery power predefined by EV owners and PVCS operators.

Power injection during V2G mode is constrained by eq. (50), EV is allowed to inject the power if and only if $P_{EV,pre}$ is greater than the $P_{EV,crit}$ and a_1 percentage of $P_{EV,max}$, here, a_1 is defined by the EV owners. Fast charging of the EVs is stopped completely and slow charging is also stopped if eq. (51) is not satisfied. EV charging is shifted from fast charging to slow charging if eq. (52) is satisfied and charging is stopped if eq. (53) is satisfied. Eq. (51) is the overriding constraint for both eq. (52) and eq. (53). The charging constraints are applied during the system failures and unavailability of main grid supply.

C. OPTIMIZATION TECHNIQUE

1) Grasshopper optimization algorithm

The Grasshopper optimization algorithm (GOA) [32] replicates the swarming behaviour of grasshoppers in the natural world, and its mathematical equations and formulas are presented as follows. The position of the grasshopper is expressed as

$$X_i = S_i + G_i + A_i \tag{54}$$

here, X_i is the position of the i^{th} grasshopper. S_i, G_i and A_i are the social interaction, gravity force and wind advection respectively.

The social interaction of the grasshoppers is modeled as

$$S_i = \sum_{j=1, j\neq i}^{N} s(d_{ij})\widehat{d_{ij}} \tag{55}$$

where, N= total number of grasshoppers. d_{ij}= distance between i^{th} and j^{th} grasshoppers and is calculated by $d_{ij} = |x_j - x_i|$. $\widehat{d_{ij}}$ = unit vector of i^{th} grasshopper and is calculated by $(x_j - x_i)/d_{ij}$. s is the function that defines the strength of social force and is expressed as

$$s(k) = fe^{-k/)} - e^{-k} \tag{56}$$

here, f and l are the attractive intensity and length scale respectively.

The gravity force is calculated by

$$G_i = -g\widehat{e_g} \tag{57}$$

where g = gravitational constant and $\widehat{e_g}$ = unity vector towards the centre of earth.

The wind advection is calculated by

$$A_i = u\widehat{e_w} \tag{58}$$

here, where u = constant drift and $\widehat{e_w}$ = unity vector in the direction of wind.

Now, rewrite the eq.(54) by substituting the eq.(55), eq.(57) and eq.(58)

$$X_i = \sum_{j=1, j\neq i}^{N} s(|x_j - x_i|)\left(\frac{x_j - x_i}{d_{ij}}\right) - g\widehat{e_g} + u\widehat{e_w} \tag{59}$$

Any stochastic algorithm has to perform exploration and exploitation efficiently to solve the optimization problems to get global optimum solution. Some special parameters are integrated with eq.(59) to show the exploration and exploitation in the optimization process. The mathematical model is expressed as

$$X_i = c\left(\sum_{j=1, j\neq i}^{N} c\frac{UB_d - LB_d}{2} s(|x_j - x_i|)\frac{x_j - x_i}{d_{ij}}\right) + \widehat{T_d} \tag{60}$$

here, UB_d and LB_d are the upper and lower bounds of the d^{th} dimension respectively. $\widehat{T_d}$ is the value of d^{th} dimension target (best solution till now). c is a coefficient to shrink the comfort area, repulsion area, and attraction area.

The value of c decreases with iterations and is evaluated for each iteration. The mathematical expression for calculation of c is as follows

$$c = c_{max} - Iter\frac{c_{max} - c_{min}}{Iter_{max}} \tag{61}$$

here, c_{max} and c_{min} are the maximum and minimum values of c respectively. $Iter$ and $Iter_{max}$ are the current iteration and maximum number of iterations respectively.

2) Multi Objective Grasshopper optimization algorithm (MOGOA)

A multi objective algorithm basically has two goals i.e., firstly finding true pareto solutions and well distribution of Pareto solutions across all objectives. This is mandatory in the posteriori methods where decision making is done post optimization. Multi objective has more than one objective and hence, it is not possible to compare two solutions using regular relational operations. In MOGOA, the Pareto dominance is used to compare the solutions. The optimal Pareto solutions are stored in an archive. The main challenge is to choose the target which is the major component and leads all the search agents towards the optimal solution. The Pareto solutions are saved in the archive and target must be one of them. While selecting the target, the number of neighbouring solutions for each solution is calculated by considering a fixed distance. The probability of choosing i^{th} solution as a target (p_i) is calculated by

$$p_i = 1/N_i \tag{62}$$

here, N_i is number of solutions in the neighbourhood of i^{th} solution.

The target is selected with the help of probability and a roulette wheel. This also improves the distribution of solutions in the less distributed regions in the search space. This also helps to avoids the premature convergence by selecting the target from a crowded neighbourhood. The limitation is kept in the number of solutions stored in the archive to reduce the computational cost. When the archive is full, some of the solutions in the crowded region are removed to reduce the solutions in that region. This process allows to accommodate the new solutions in the less populated regions. This is achieved by taking the inverse of p_i and roulette wheel. The archive is continuously updated by considering different cases, since, archive stores non-dominated solution so any non-dominated solution is immediately added to archive. If any outside solution dominates the solution in the archive, then it must be replaced.

The flow chart of the proposed optimal placement of PVCS is shown in Fig. 6.

The archive has all the non-dominated solutions. Final decision should be taken after the optimization process ends. In this work, the compromised solution is determined using Euclidean distance method and Euclidean distance (ED) of i^{th} solution is calculated by

$$ED_i = \sqrt{Obj_{1,i}^2 + Obj_{2,i}^2} \tag{63}$$

The compromised solution is selected which is having minimum ED.

IV. RESULTS AND DISCUSSIONS

The proposed methodology is hypothetically applied on a practical Indian distribution system. The serving area of the distribution system 15 km^2 which includes urban and semi-urban areas in Silchar town, Assam India. The pictorial representation of the system is shown in Fig. 7. The distribution system is served by a single substation (33/11 kV) and a medium voltage (11 kV) the radial feeders. The feeders are divided into different feeder sections and loads of each feeder section is assumed to be concentrated at one point called as load bus. The test system has total 60 buses i.e., 59 load buses and one substation bus. Total of 6440 low voltage consumers are connected to the system with a peak demand of 17.45 MW and 5 medium voltage consumers with a 10 MW contractual demand. The estimated vehicles in the serving area are 3864 which gives approximately 0.6 vehicles per consumer. The substation capacity is assumed to be upgraded to meet the new EV charging load. To simplify the analysis of PVCS impact on the distribution system, the load on the distribution system is considered as constant for reliability analysis.

The basic idea of PVCS is to utilize the rooftops of the buildings to install solar PV systems and integrate to the

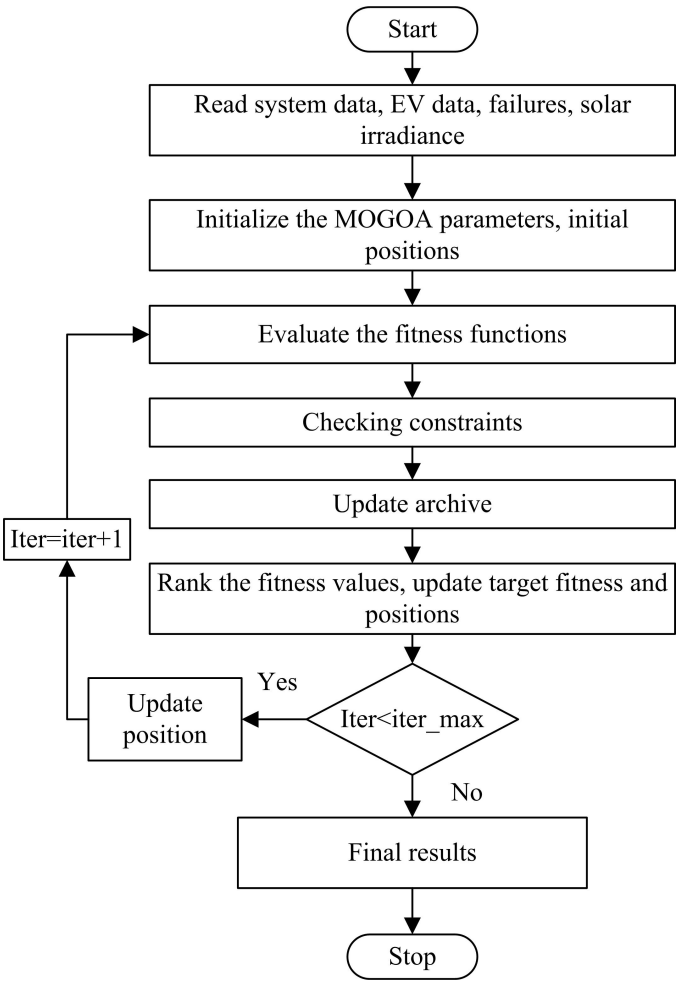

FIGURE 6. Flow chart for placement of PVCS using MOGOA

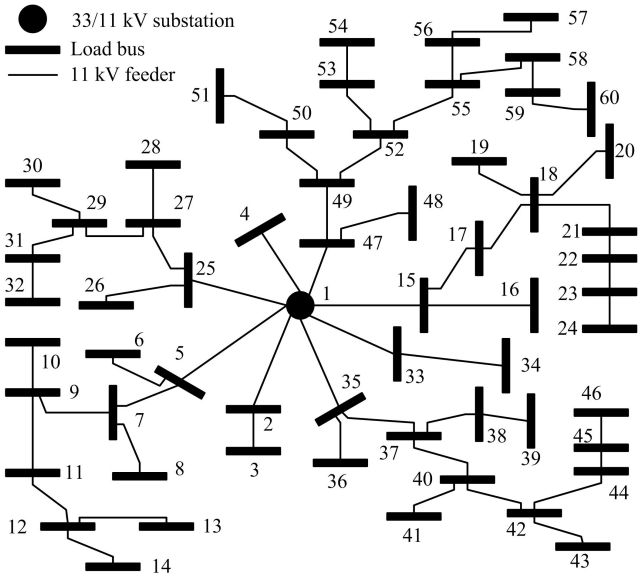

FIGURE 7. Test distribution system

charging station. The PV output from the different buildings is pooled and connected to the distribution system at a particular bus. The PVCS is distributed and controlled centrally which removes the need of higher land requirement at single place as it is very tough to get in the urban areas. In this work, three different EV penetration levels are considered i.e., 35%, 50% and 60% for PVCS placement. The charging station is installed within the residential area, so that parking area of residential building is used for the same purpose. The system operators also allowed the EV owners to install slow charging ports at their homes if PVCS is not available near to their house. The charging of the EV depends on several parameters such as initial battery level, duration of travel, arrival time etc. In this work, initial battery levels are randomly generated by considering $P_{EV,cri}$ as lower limit and $P_{EV,max}$ as upper limit. The travel distance and arrival times are assumed arbitrarily. The arrival times are ensuring the number of vehicles connected to PVCS at any instant. The charge requirement is evaluated with the help of travel distance and charging mode is decided based on the initial battery level, required battery level. The percentage of EVs in different modes in a typical day is shown in Fig. 8.

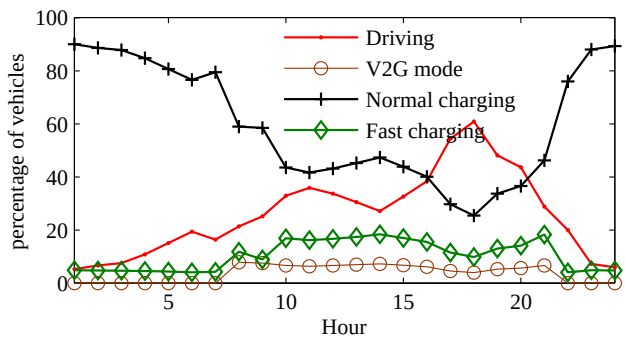

FIGURE 8. Percentage of EVs in Charging, discharging and driving mode

The system reliability is evaluated using Monte Carlo simulation. The distribution system component failures are randomly simulated and repair and replacement timings are generated randomly for each component failure. Only EENS value is used to describe the system reliability. The solar irradiance data is collected from [33] for a year and the same data is used to generate the solar PV output power for one year. The solar PV output power for a typical day is shown in Fig. 9 and the output power is mentioned in p.u values.

In this work, total five PVCSs are simultaneously placed to improve the system reliability and EVs reliability as well which means PVCS placement is solved as multi-objective problem. The PVCS placement problem is solved using a multi-objective Grasshopper optimization algorithm (MOGOA) for different EV penetration levels. The effectiveness of MOGOA is compared with multi-objective ant lion optimization (MOALO) algorithm. The population size and maximum iterations are taken as 30 and 50 respectively

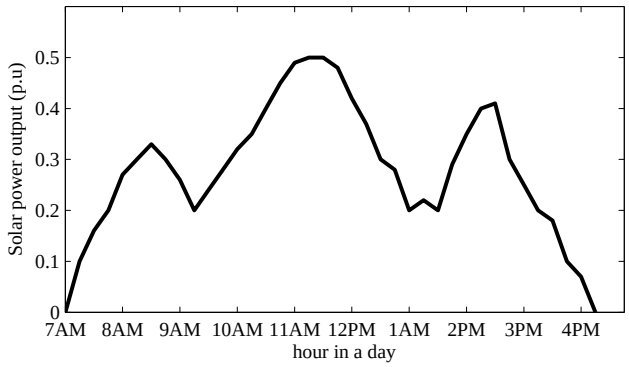

FIGURE 9. Solar output power in a day

for both the algorithms for all the conditions. To simplify the results discussion, different cases are considered which are given below

1) *Base case:* In this case, the system reliability is evaluated without EV charging and rooftop PV systems.
2) *Case 1:* Five EV charging stations are simultaneously placed without rooftop PV systems.
3) *Case 2:* In this case, five PVCSs are simultaneously placed in the distribution system.

The EENS value for base case is 83.91 MWh. The pareto optimal solutions for case 1 and 35% EV penetration level is shown in Fig. 10 for different algorithms. The compromised solutions are found using eq.(63) and illustrated in the Fig. 10.

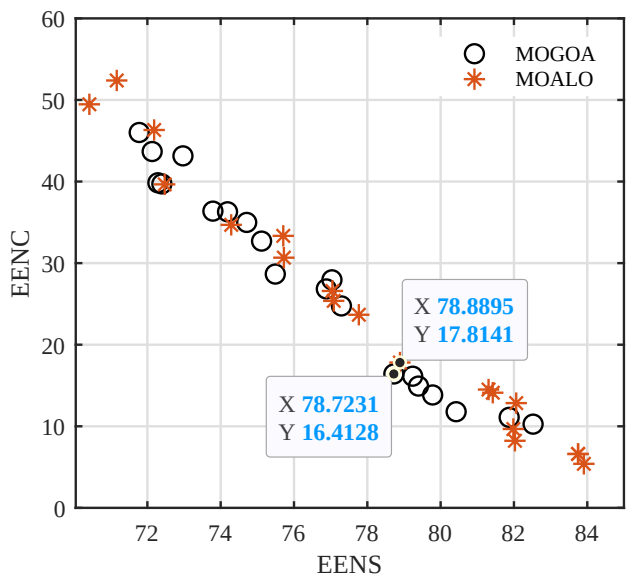

FIGURE 10. Pareto optimal solutions for case 1 with 35% EV penetration

The values of objective functions and CS locations for compromised solution is given Table 1 for both algorithms and 35% EV penetration level. From the Table 1, it is observed that 2 CS are placed at same locations with both the methods and remaining are placed at different locations. The MOGOA giving better reliability as compared to MOALO algorithm. However, there is not a much difference with EENS value and considerable difference is found in EENC values. EENC is better with MOGOA algorithm.

TABLE 1. Optimal solution for case 1 with 35% EV penetration

	EENS	EENC	CS locations
MOGOA	78.723	16.41	7, 16, 26, 38, 53
MOALO	78.889	17.81	7, 20, 29, 36, 53

The observations from the Table 1 are as follows, the EENS value is reduced by 6.18% and 5.98% with reference to base case for MOGOA and MOALO respectively.

The pareto optimal solutions for case 2 and 35% EV penetration level is shown in Fig. 11 for different algorithms. The compromised solutions are found using eq.(63) and illustrated in the Fig. 11.

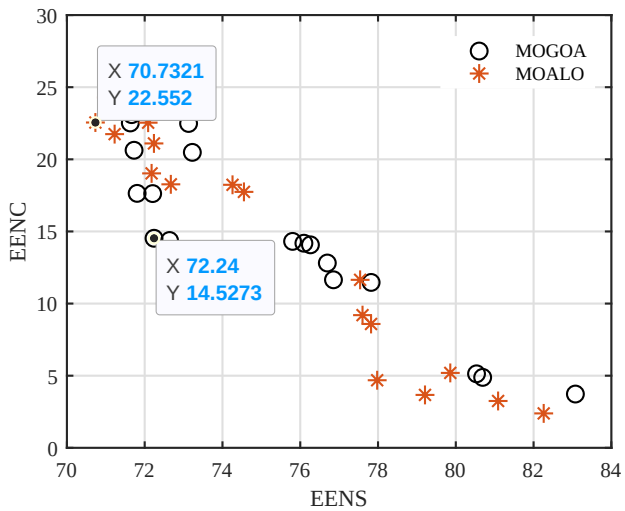

FIGURE 11. Pareto optimal solutions for case 2 with 35% EV penetration

The values of objective functions and PVCS locations and size for compromised solution is given in Table 2 for both algorithms and 35% EV penetration level. One of the PVCS location is same as case 1 for both the methods. In case, total 3 PVCS are placed at same locations for both the algorithms. The total installed capacity of solar PV systems is 29.3 MW and 28.1 MW for MOGOA and MOALO algorithms respectively. The EENS is better with MOALO as compared to MOGOA but EENC is highly compromised.

TABLE 2. Optimal solution for case 2 with 35% EV penetration

	EENS	EENC	PVCS locations	PVCS Size (MW)
MOGOA	72.24	14.527	13, 16, 32, 44, 53	8.8, 5.3, 9.5, 1.9, 3.8
MOALO	70.732	22.551	13, 19, 32, 37, 53	6.9, 3.7, 5.7, 8.4, 3.4

The observations from the Table 2, are as follows, the EENS value is reduced by 13.9% and 15.7% with reference

to base case for MOGOA and MOALO respectively. The EENC value is reduced by 11.52% and increased by 26.61% in case 2 as compared to case 1 for MOGOA and MOALO respectively.

The detailed EV reliability evaluation and energy injected by EVs in different conditions are given in Table 3 for both case 1 and 2. The EENC has two components i.e., due to not charged and unscheduled energy injection (V2G mode).

TABLE 3. Comparison of EENC with 35% EV penetration

EENC		Not Charged	V2G (Unscheduled)	Total
Case 1	MOGOA	9.588	6.824	16.413
	MOALO	13.355	4.459	17.814
Case 2	MOGOA	9.852	4.674	14.527
	MOALO	15.555	6.996	22.551

As observed from Table 3, EENC value is reduced in case 2 with MOGOA but increased with MOALO algorithm. The component of not charged has negligible increment in case 2 for MOGOA, whereas, considerable increase is found with MOALO algorithm. In case 1, the unscheduled energy injection is more with MOGOA algorithm and reduced in case 2. However, unscheduled energy injection is increased in case 2 with MOALO. The MOGOA shown it's superiority in improving EENC.

The energy injection in V2G is shown in Table 4 for both the cases and algorithms. The scheduled injection is same in case 1 with both algorithms. In case 2, PV output helped the EVs to inject more energy from the scheduled V2G mode. In case 2, scheduled injected energy is more with MOALO algorithm. The more scheduled injected energy helped to improve the system reliability which is observed in Table 2, where, MOALO algorithm giving better EENS. The unscheduled energy injection is reduced in case 2 with MOGOA, whereas, increased with MOALO algorithm. The less unscheduled energy injection improved the EENC which is witnessed in Table 2.

TABLE 4. Energy injection of V2G mode with 35% EV penetration

Energy Injected		Scheduled	Unscheduled	Total
Case 1	MOGOA	3.859	6.824	10.684
	MOALO	3.859	4.459	8.319
Case 2	MOGOA	7.776	4.674	12.451
	MOALO	13.207	6.996	20.204

The change in EENS and EENC is given in Table 5 for 35% EV penetration and MOGOA algorithm. The '-' and '+' denotes decrease and increase of values in case 2 respectively. The reduction in EENC is more as compared to EENS. The scheduled energy injection is drastically increased whereas, unscheduled energy injection is reduced in case 2. Overall, injected energy is increased and the unscheduled component of it is decreased. It is a clear indication that PV integration with charging station is improving system reliability as well as EV reliability.

TABLE 5. Comparison of reliability for 35% EV penetration for MOGOA

Reliability		Case 1	Case 2	Change (%)
EENS		78.723	72.24	-8.2
EENC	Not charged	9.588	9.852	+2.7
	V2G (Unscheduled)	6.824	4.674	-31.5
	Total	16.412	14.527	-11.4
Energy Injected	Scheduled	3.859	7.776	+101.4
	Unscheduled	6.824	4.674	-31.5
	Total	10.684	12.451	+16.5

The PVCSs are optimally placed by considering 50% and 60% EV penetration levels without changing the distribution system load and the system outage conditions remain same as 35% EV penetration level. The MOGOA is used for the PVCS placement. The reliability values, optimal locations and sizes are given in Table 6 for case 2. From the Table 6,

TABLE 6. Optimal solution for case 2 with 50% and 60% EV penetration

EV Level	EENS	EENC	PVCS locations	PVCS Size (MW)
50%	72.782	23.813	13, 19, 28, 33, 53	10, 9.7, 5.4, 3.7, 1.1
60%	76.192	24.522	11, 16, 28, 34, 52	7.5, 9.0, 9.2, 6.0, 5.8

it is observed that system reliability is reduced considerably, whereas, EV reliability is reduced less comparatively. The PV installed capacity is 29.9 MW and 37.7 MW for 50% and 60% EV penetration level respectively.

The different components of EENC value are given in Table 7 for 50% and 60% EV penetration levels. It is found that there is no considerable difference between both the components i.e., not charged and unscheduled V2G mode values.

TABLE 7. EENC values for 50% and 60% EV penetration

EV Level	Not Charged	V2G (Unscheduled)	Total
50%	18.18	5.632	23.813
60%	18.842	5.68	24.522

The energy injection by V2G mode of EV under different condition is given in Table 8. From the Table 8, it is found that changes in scheduled and unscheduled energy injection is negligible while changing the EV penetration level from 50% to 60%.

TABLE 8. Energy injection of V2G mode for 50% and 60% EV penetration

EV Level	Scheduled	Unscheduled	Total
50%	13.741	5.632	19.374
60%	13.485	5.68	19.166

The comparison of reliability and total PV installed capacity for three EV penetration levels is given in Table 9. The relative change of EENS is higher if EV penetration level is increased. But at the same time, the relative change in EENC is less with increased EV penetration level. From 35% to 50%, total installed PV capacity with charging

station doesn't change much. Whereas, a drastic change is found from 50% to 60%.

TABLE 9. Reliability and PV installed capacity for different penetration levels

EV Level	EENS	EENC	PV capacity (MW)
35%	72.24	14.527	29.3
50%	72.782	23.813	29.9
60%	76.192	24.522	37.7

The rooftop required for 1 MW solar PV system is 5 acres. The serviceable area of the studied distribution system is 3706 acres (15 km^2). The 60% EV penetration requires 190 acres of rooftop which is approximately 5.1% of total serviceable area of the distribution system.

V. CONCLUSION

In this paper, multiple solar rooftop PV integrated charging stations are optimally placed in the distribution system for reliability benefits. Along with the system reliability index, EV reliability index is also considered as an objective for PVCS placement. A novel index for EV reliability i.e., expected energy not charged (EENC) is developed and used as an objective function. Hence, the PVCS placement problem is solved as a multi-objective problem using MOGOA and results are compared with MOALO algorithm. The PVCS are hypothetically placed in a practical distribution system and 0.6 vehicles per consumer are considered. Three different EV penetration levels are considered for impact analysis while keeping system load constant. The reliability is compared with and without PV integration to the charging stations. The V2G mode (scheduled & unscheduled) has improved the system reliability in case 1 as this mode works as generating mode. The integration of rooftop solar PV systems in the charging station further improved the system reliability and EV reliability as well. The contribution of not charging EVs in EENC has negligible change with PV integration whereas unscheduled V2G mode contribution is reduced and leads to improving the EV reliability. The energy injection from the scheduled V2G mode is increased with PVCS and contributed in improving system reliability. The system reliability is reducing with increase of EV penetration level. The relative change in EENC is less at higher penetration levels as compared to lower penetration levels. The area required for installing rooftop solar PV system is approximately 5.1% of distribution system serviceable area which is very well possible limit.

The proposed methods are easily scalable to apply for large and complex systems. In this work, tariff rates for charging and V2G mode of EVs is not considered. The participation of EVs is fully based on the minimum battery levels predefined by EV owners. However, if time of use tariff are applied then this will encourage the EV owners to participate in V2G mode during high tariff durations and charge their EVs during low tariff durations. The impact of time of use tariff has to be analysed in the future works. The use of fuel cells as DG is increasing in recent time and it is very interesting to analyse the impact of fuel cells and PVCS on the system and EV reliability.

REFERENCES

[1] J. D. Kim and M. Rahimi, "Future energy loads for a large-scale adoption of electric vehicles in the city of los angeles: Impacts on greenhouse gas (GHG) emissions," *Energy Policy*, vol. 73, pp. 620 – 630, 2014.

[2] G. Alkawsi, Y. Baashar, D. Abbas U, A. A. Alkahtani, and S. K. Tiong, "Review of renewable energy-based charging infrastructure for electric vehicles," *Applied Sciences*, vol. 11, no. 9, 2021.

[3] G. H. Reddy, M. K. Kiran, P. S. Kumar, A. K. Goswami, and N. B. D. Choudhury, "Fuzzy reliability assessment of distribution system with wind farms and plug-in electric vehicles," *Electric Power Components and Systems*, vol. 47, no. 19-20, pp. 1791–1804, 2019.

[4] M. Safayatullah, M. T. Elrais, S. Ghosh, R. Rezaii, and I. Batarseh, "A comprehensive review of power converter topologies and control methods for electric vehicle fast charging applications," *IEEE Access*, vol. 10, pp. 40 753–40 793, 2022.

[5] K. Y. Yap, H. H. Chin, and J. J. Klemes, "Solar energy-powered battery electric vehicle charging stations: Current development and future prospect review," *Renewable and Sustainable Energy Reviews*, vol. 169, p. 112862, 2022.

[6] S. S. Deshmukh and J. M. Pearce, "Electric vehicle charging potential from retail parking lot solar photovoltaic awnings," *Renewable Energy*, vol. 169, pp. 608–617, 2021.

[7] K. Kathiravan and P. Rajnarayanan, "Application of aoa algorithm for optimal placement of electric vehicle charging station to minimize line losses," *Electric Power Systems Research*, vol. 214, p. 108868, 2023.

[8] S. Mateen, A. Haque, V. S. B. Kurukuru, and M. A. Khan, "Discrete stochastic control for energy management with photovoltaic electric vehicle charging station," *CPSS Transactions on Power Electronics and Applications*, vol. 7, no. 2, pp. 216–225, 2022.

[9] C. Sun, X. Zhao, B. Qi, W. Xiao, and H. Zhang, "Economic and environmental analysis of coupled pv-energy storage-charging station considering location and scale," *Applied Energy*, vol. 328, p. 119680, 2022.

[10] V. Jain, S. Kewat, and B. Singh, "Three phase grid connected pv based ev charging station with capability of compensation of reactive power," *IEEE Transactions on Industry Applications*, vol. 59, no. 1, pp. 367–376, 2023.

[11] H. R. Galiveeti, A. K. Goswami, and N. B. D. Choudhury, "Impact of plug-in electric vehicles and distributed generation on reliability of distribution systems," *Engineering Science and Technology, an International Journal*, vol. 21, no. 1, pp. 50 – 59, 2018.

[12] M. T. Turan, Y. Ates, O. Erdinc, E. Gokalp, and J. P. Catalão, "Effect of electric vehicle parking lots equipped with roof mounted photovoltaic panels on the distribution network," *International Journal of Electrical Power & Energy Systems*, vol. 109, pp. 283–289, 2019.

[13] G. J. Osório, M. Gough, M. Lotfi, S. F. Santos, H. M. Espassandim, M. Shafie-khah, and J. P. Catalão, "Rooftop photovoltaic parking lots to support electric vehicles charging: A comprehensive survey," *International Journal of Electrical Power & Energy Systems*, vol. 133, p. 107274, 2021.

[14] A. K. Barnwal, L. K. Yadav, and M. K. Verma, "A multi-objective approach for voltage stability enhancement and loss reduction under pqv and p buses through reconfiguration and distributed generation allocation," *IEEE Access*, vol. 10, pp. 16 609–16 623, 2022.

[15] M. Ali Shaik, P. L. Mareddy, and V. N., "Enhancement of voltage profile in the distribution system by reconfiguring with dg placement using equilibrium optimizer," *Alexandria Engineering Journal*, vol. 61, no. 5, pp. 4081–4093, 2022.

[16] G. H. Reddy, A. N. Koundinya, S. Gope, M. Raju, and K. M. Singh, "Optimal sizing and allocation of dg and facts device in the distribution system using fractional lévy flight bat algorithm," *IFAC-PapersOnLine*, vol. 55, no. 1, pp. 168–173, 2022, 7th International Conference on Advances in Control and Optimization of Dynamical Systems ACODS 2022.

[17] R. Kizito, X. Li, K. Sun, and S. Li, "Optimal distributed generator placement in utility-based microgrids during a large-scale grid disturbance," *IEEE Access*, vol. 8, pp. 21 333–21 344, 2020.

[18] S. Dharmasena, T. O. Olowu, and A. I. Sarwat, "Algorithmic formulation for network resilience enhancement by optimal der hosting and placement," *IEEE Access*, vol. 10, pp. 23 477–23 488, 2022.

[19] G. H. Reddy, P. Chakrapani, A. K. Goswami, and N. B. D. Choudhury, "Optimal distributed generation placement in distribution system to improve reliability and critical loads pick up after natural disasters,"

Engineering Science and Technology, an International Journal, vol. 20, no. 3, pp. 825 – 832, June 2017.

[20] F. Borousan and M.-A. Hamidan, "Distributed power generation planning for distribution network using chimp optimization algorithm in order to reliability improvement," *Electric Power Systems Research*, vol. 217, p. 109109, 2023.

[21] H. M. A. Ahmed, H. F. Sindi, M. A. Azzouz, and A. S. A. Awad, "Optimal sizing and scheduling of mobile energy storage toward high penetration levels of renewable energy and fast charging stations," *IEEE Transactions on Energy Conversion*, vol. 37, no. 2, pp. 1075–1086, 2022.

[22] W. S. Tounsi Fokui, M. J. Saulo, and L. Ngoo, "Optimal placement of electric vehicle charging stations in a distribution network with randomly distributed rooftop photovoltaic systems," *IEEE Access*, vol. 9, pp. 132 397–132 411, 2021.

[23] R. Chowdhury, B. K. Mukherjee, P. Mishra, and H. D. Mathur, "Performance assessment of a distribution system by simultaneous optimal positioning of electric vehicle charging stations and distributed generators," *Electric Power Systems Research*, vol. 214, p. 108934, 2023.

[24] M. Bilal, M. Rizwan, I. Alsaidan, and F. M. Almasoudi, "Ai-based approach for optimal placement of evcs and dg with reliability analysis," *IEEE Access*, vol. 9, pp. 154 204–154 224, 2021.

[25] A. Asaad, A. Ali, K. Mahmoud, M. F. Shaaban, M. Lehtonen, A. M. Kassem, and M. Ebeed, "Multi-objective optimal planning of ev charging stations and renewable energy resources for smart microgrids," *Energy Science & Engineering*, vol. 11, no. 3, pp. 1202–1218, 2023.

[26] A. Ali, M. F. Shaaban, A. Abdelfatah, M. A. Azzouz, and A. S. Awad, "Optimal allocation of fcss and pv units in smart grids considering traffic and generation dispatch," *Sustainable Energy, Grids and Networks*, vol. 34, p. 101063, 2023.

[27] A. Ali, M. F. Shaaban, A. S. A. Awad, M. A. Azzouz, M. Lehtonen, and K. Mahmoud, "Multi-objective allocation of ev charging stations and ress in distribution systems considering advanced control schemes," *IEEE Transactions on Vehicular Technology*, vol. 72, no. 3, pp. 3146–3160, 2023.

[28] W. S. Tounsi Fokui, M. J. Saulo, and L. Ngoo, "Optimal placement of electric vehicle charging stations in a distribution network with randomly distributed rooftop photovoltaic systems," *IEEE Access*, vol. 9, pp. 132 397–132 411, 2021.

[29] S. Z. Mirjalili, S. Mirjalili, S. Saremi, H. Faris, and I. Aljarah, "Grasshopper optimization algorithm for multi-objective optimization problems," *Applied Intelligence*, vol. 48, pp. 805–820, August 2018.

[30] A. Singla, K. Singh, and V. K. Yadav, "Optimization of distributed solar photovoltaic power generation in day-ahead electricity market incorporating irradiance uncertainty," *Journal of Modern Power Systems and Clean Energy*, vol. 9, no. 3, pp. 545–560, 2021.

[31] M. K N and J. E A, "Optimal integration of distributed generation (dg) resources in unbalanced distribution system considering uncertainty modelling," *International Transactions on Electrical Energy Systems*, vol. 27, no. 1, p. e2248, 2017, e2248 ETEP-15-0869.R1.

[32] S. Saremi, S. Mirjalili, and A. Lewis, "Grasshopper optimisation algorithm: Theory and application," *Advances in Engineering Software*, vol. 105, pp. 30–47, 2017.

[33] (2022) CFSR global weather data for SWAT. [Online]. Available: https://swat.tamu.edu/data/cfsr

GALIVEETI HEMAKUMAR REDDY (M'2013) was born in Kadapa, Andhra Pradesh, India, in 1989. He received the B.Tech. degree in electrical and electronics engineering and the M.Tech. degree in electrical power systems from the Madanapalle Institute of Technology and Science, Madanapalle, India, in 2010 and 2012, respectively, and the Ph.D. degree in electrical engineering from the National Institute of Technology at Silchar, Silchar, India, in 2018. He is currently an Associate Professor with the Department of Electrical Engineering, DPG Institute of Technology and Management, Gurugram, India. His current research interests include distribution system reliability, power quality assessment and mitigation, damage assessment, electric vehicles integration, distribution system restoration, and fuzzy applications in power systems.

He is a member of the IEEE PES Society and the IEEE Smart Grid Society. He is also a Frequent Reviewer of the IEEE TRANSACTIONS ON SMART GRID, the IEEE TRANSACTIONS ON INDUSTRY APPLICATION, the IEEE TRANSACTIONSON RELIABILITY, Electrical Power Systems Research, and several other international journals.

SHOBHA RANI DEPURA (M'2020) received her B.E degree in Electrical and Electronics Engineering from Jawaharlal Nehru Technology University, Hyderabad, and M.Tech. degree in Power System from Sri Venkateswara University Tirupathi, India. Dr. Shobha has completed her Ph.D. degree at Sri Venkateswara University, Tirupathi. Currently she is working as a Professor in the department of Electrical and Electronics Engineering at Institute of Aeronautical Engineering, Hyderabad, India. Her areas of interest include control systems and application of power Systems and Power electronics.

SADHAN GOPE (M'2012–SM'2022) is presently working as an Assistant Professor in the Department of Electrical Engineering, National Institute of Technology Agartala. Before joining National Institute of Technology Agartala, he was a faculty member of Mizoram University and National Institute of Technology Mizoram. He has completed his Ph.D. in Electrical Engineering from National Institute of Technology Silchar, India, Master of Technology in Power and Energy System Engineering from National Institute of Technology, Silchar, India, Bachelor of Engineering in Electrical and Electronics Engineering from National Institute of Technology, Agartala, India. He has published more than 60 papers in International Journals and Conference Proceedings. He is a regular reviewer of different International Journals and various conferences. He is a lifetime member of Indian Society of Technical Education (ISTE) and member of The Institution of Engineers (India), Automatic Control and Dynamical Optimization Society (ACDOS) and International Association of Engineers (IAENG).

He participated in many international conferences as Organizing Chair, Session Chair and member of the Technical Program Committee. His research interest areas are restructured electricity market, transmission congestion management, distributed and renewable energy generation, hybrid energy systems, application of soft computing techniques in power system.

BALLEKURA VEERA NARAYANA was born in India on June 15, 1987. He received B.Tech Degree in Electrical and Electronics Engineering from VRS and YRN College of engineering and technology Andhra Pradesh, in 2008, India. He completed M.Tech degree in Power Electronics and Electric Drives from Vignan's Engineering College, Vadlamudi in 2011, India. Presently he is a working as Assistant Professor in Aditya Engineering College. His research interests include Power Electronics, Electrical Drives, FACT devices and Integrated Renewable Energy Systems.

MURALIDHAR NAYAK BHUKYA (M'2015) was born in 1987, India. He received the B.Tech. degree in electrical and electronics engineering and the M.Tech. degree in power electronics from Jawaharlal Nehru Technological University, Hyderabad, India, in 2008 and 2013, respectively, and the Ph.D. degree in electrical and electronics engineering from Jawaharlal Nehru Technological University, Kakinada. He is currently working as an Assistant Professor with the Department of Electrical Engineering, School of Engineering and Technology, Central University of Haryana, India. His research interests include control systems, special machines, and application of power electronics in renewable energy systems.